Optimization of Spot-Welded Joints Combined Artificial Bee Colony Algorithm with Sequential Kriging Optimization

Article *in* Advances in Mechanical Engineering · August 2014

DOI: 10.1155/2014/573694

Jianguang Fang
University of Sydney

Yunkai Gao
Tongji University

Guangyong Sun
University of Sydney

Qing Li
University of Sydney

Hindawi Publishing Corporation
Advances in Mechanical Engineering
Volume 2014, Article ID 573694, 10 pages
http://dx.doi.org/10.1155/2014/573694

Research Article

Optimization of Spot-Welded Joints Combined Artificial Bee Colony Algorithm with Sequential Kriging Optimization

Jianguang Fang,[1,2] Yunkai Gao,[1] Guangyong Sun,[3] Chengmin Xu,[1] Yuting Zhang,[1] and Qing Li[2]

[1] *School of Automotive Studies, Tongji University, Shanghai 201804, China*
[2] *School of Aerospace, Mechanical and Mechatronic Engineering, The University of Sydney, Sydney, NSW 2006, Australia*
[3] *State Key Laboratory of Advanced Design and Manufacture for Vehicle Body, Hunan University, Changsha 410082, China*

Correspondence should be addressed to Yunkai Gao; gaoyunkai@tongji.edu.cn and Guangyong Sun; sgy800@126.com

Received 29 March 2014; Accepted 23 June 2014; Published 4 August 2014

Academic Editor: Sandra Velarde-Suárez

Generally, spot-welded joints are the weakest parts of structures leading to fatigue failure under fluctuating loads. Therefore, it is important to optimize the spot weld to improve the fatigue life. However, a classical optimization of the spot weld often directly couples finite element analysis (FEA) with optimization algorithm, which may fall into a local optimum or be expensive computationally. In this study, a metamodel-based optimization procedure is proposed to find the optimum locations of spot-welded joints for maximum fatigue life. Based on the initial training points, Kriging model is implemented to approximate the objective function regarding the design variables (i.e., locations of spot welds). To further overcome the defect of traditional Kriging model and improve the accuracy of optimum results, the sequential Kriging optimization (SKO) is utilized, where the Kriging model is updated iteratively by adding new training points to the training dataset till the global optimum is obtained. The optimization is run using artificial bee colony (ABC) algorithm and the results show that our proposed method is able to improve the performance of the spot-welded joint. More importantly, more competent optimum can be found and the optimization can be executed more efficiently, compared to the conventional methods.

1. Introduction

Automotive bodies as many other structures are composed of metal sheets joined by spot welds. There are about 4,000–6,000 spot welds in a typical body in white (BIW). Because spot weld joints provide localized connection and thus lead to high stress concentration in the joined plates, any improper design may result in excessively high stresses and premature failure [1]. Among these failure modes, fatigue is the most failure mode. It is imperative for automotive engineers to understand fatigue behavior of spot-welded joints under fluctuating loads. In this regard, numerical techniques have been developed to carry out the predictive tasks such as design, analysis, and evaluation. For example, Deng et al. [2] studied the mechanical behavior of spot welds under tensile-shear and symmetric coach-peel loading conditions using finite element analysis (FEA). Pan and Sheppard [3] presented a strain-based approach which could predict the fatigue life of mixed-thickness spot welds well based on empirical fatigue life data and FEA. Mahadevan and Ni [4] developed a damage tolerance reliability analysis method for automotive spot-welded joints using a three-dimensional finite element (FE) model. Wang and Shang [5] carried out elastoplastic FEA for a single spot tensile-shear spot weld and predicted the low-cycle fatigue life. Ertas et al. [6] took into account the material nonlinearity, local plastic deformations around the welds during loading, and the residual stress and strain after unloading in FEA. Based on the predicted stress and strain states, fatigue lives were calculated and compared to experimental results. Tovo and Livieri [7] adopted an implicit gradient approach to investigate the fatigue strength of spot welds, where the material was assumed linear elastic and an effective stress for the fatigue life estimation was considered as a transformation of the maximum principal stress field.

Zhang and Taylor [8] pointed out that the fatigue indictors could be a complex function of spot weld positions, even in the simple two-spot case. In addition, the fatigue indictors may be very sensitive to the design parameters such as the spot weld positions. For these reasons, the design optimization of spot-welded structures could be very helpful and beneficial in engineering applications. In this regard, Zhang and Taylor [8] introduced an umbrella model of spot welds and the radial stresses around a spot weld into the optimization process of fatigue life. Chae et al. [9] proposed an optimal design system for spot welding locations in shell structures, where an h-version of adaptive meshing scheme based on background mesh was implemented. Ertas and Sonmez [10] integrated the design optimization procedure with commercial software ANSYS to minimize the maximum Von Mises stress, where the Nelder-Mead simplex method was used to change the locations iteratively. Later, they also applied this procedure to find the optimal locations of spot welds and the optimal overlapping length of the joined plates to maximize fatigue life for a number of cases [1].

These abovementioned studies on optimization of spot-welded joints are restricted to directly coupling numerical simulation with optimization algorithm, which is commonly regarded as an inefficient way since traditional optimization usually needs to call for a lot of finite element analysis results. To address this issue, the technique of metamodels or surrogate models appears effective to replace costly simulations for optimization [11–14]. This approach establishes an approximation mathematical relationship between design variables and functional responses with a moderate number of FEA runs. Furthermore, although surrogate approximation is an effective alternative to reducing simulation time, a key issue is how to achieve a good accuracy of the surrogate model with minimum number of training points. Conventional one-step sampling strategy appears less flexible, in which the training points are generated prior to construction of metamodel and cannot be changed during the searching process in optimization. A more reliable approach is to use the sequential sampling strategy to update the metamodel iteratively during optimization until the model is sufficiently accurate and the optimization process is properly converged. The sequential sampling strategy allows taking the advantage of information gathered from previous iterations; thus the metamodel can be improved with newly generated training points in a sequential way until the accuracy of the updated metamodel becomes satisfactory.

Regarding optimization algorithms, the population-based methods like genetic algorithm (GA), particle swarm optimization (PSO), and artificial bee colony (ABC) algorithm are preferable to address engineering problems, because they do not need gradient information and are more likely to obtain global optimum. However, they are expensive in terms of computational time if directly coupled with simulation model. Fortunately, combining them with the abovementioned metamodeling approach can resolve this issue. Among those optimization algorithms, the ABC algorithm is one of the most recently introduced algorithms and its performance has been well recognized. Compared with other population-based algorithms it requires fewer control parameters. Due to its simplicity and ease of implementation, ABC has drawn considerable attention and has been successfully applied in many research areas recently [15–20]. Despite increasing awareness of the outstanding performance that the ABC algorithm offers, there has been no published work available to use it for optimization design of spot-welded joints to date. The paper will demonstrate the capacity of the ABC incorporating with sequential Kriging optimization for the design of spot-welded joints. The results show a significant improvement in both computing efficiency and precision for such a sophisticated practical design problem.

The remainder of this paper is organized as follows. Section 2 introduces the ABC algorithm. In Section 3, the theory of Kriging model and sequential sampling is presented. Section 4 provides the optimization problem for a spot-welded joint and Section 5 presents the results and discussions. Finally, the conclusion is drawn in Section 6.

2. Artificial Bee Colony Algorithm

Recently, the artificial bee colony (ABC) algorithm has drawn increasing attention for its high performance in solving various engineering problems. In this study, the ABC algorithm is used as an optimizer for design of spot-welded joints. The artificial bee colony algorithm introduced by Karaboga [21, 22] is a more recently introduced optimization algorithm that simulates the intelligent foraging behavior of honey bee swarm. In the ABC algorithm, the position of a food source represents a possible solution to the optimization problem and the nectar amount of a food source corresponds to the quality (fitness) of the associated solution. To obtain an optimum, the foraging artificial bees are divided into three groups according to their roles, namely, employed bees, onlooker bees, and scout bees. In the colony, one half consists of employed bees, and the other half includes onlooker bees. For every food source, there is only one employed bee. In other words, the number of employed bees is equal to the number of food sources around the hive. The main steps for the ABC algorithm are given as follows [23, 24].

(1) Initialize swarm with SN randomly generated n-dimensional real-valued vectors in the design space. Each vector represents a food source in the population, described as $\mathbf{x}_i = \{x_{i,1}, x_{i,2}, \ldots, x_{i,n}\}$. The position of each food source is generated according to the following equation:

$$x_{i,j} = x_{\min,j} + \text{rand}(0,1)\left(x_{\max,j} - x_{\min,j}\right), \tag{1}$$

where $i = 1, 2, \ldots, \text{SN}$, $j = 1, 2, \ldots, n$. $x_{\min,j}$ and $x_{\max,j}$ represent the lower and upper bounds for dimension j, respectively.

(2) Evaluate the fitness for each food source.

(3) Generate a new food source $\mathbf{v}_i$ for each employed bee $\mathbf{x}_i$ in the neighborhood of its present position by using a solution search equation as follows:

$$v_{i,j} = x_{i,j} + \phi_{i,j}\left(x_{i,j} - x_{k,j}\right), \tag{2}$$

where $k \in \{1, 2, \ldots, \mathrm{SN}\}$ and $j \in \{1, 2, \ldots, n\}$ are randomly chosen indices, k has to be different from i, and $\phi_{i,j}$ is a random number in the range of $[-1, 1]$.

(4) Evaluate $\mathbf{v}_i$ and compare with $\mathbf{x}_i$. If the fitness of $\mathbf{v}_i$ is equal to or better than that of $\mathbf{x}_i$, $\mathbf{v}_i$ will replace $\mathbf{x}_i$ and become a new member of the population; otherwise $\mathbf{x}_i$ is retained.

(5) Share the information related to the nectar amounts and the positions of all employed bees with the onlooker bees on the dance area. Each onlooker bee selects a food source by using a fitness based probabilistic selection strategy, for example, roulette wheel selection strategy. The probabilistic value depends on the fitness values of the solutions in the population, as follows:

$$p_i = \frac{f_i}{\sum_{j=1}^{\mathrm{SN}} f_i}, \tag{3}$$

where f_i is the fitness value of solution i. Obviously, the higher the f_i is, the higher probability the ith food source is selected. Once the onlooker has selected her food source $\mathbf{x}_i$, she will produce a modification on $\mathbf{x}_i$ according to (2).

(6) Evaluate the modified food source $\mathbf{v}_i$ and compare with $\mathbf{x}_i$. If modified food source $\mathbf{v}_i$ has a better or equal nectar amount compared to $\mathbf{x}_i$, the modified food source $\mathbf{v}_i$ will replace $\mathbf{x}_i$ and become a new member in the population; otherwise $\mathbf{x}_i$ is retained.

(7) Determine the abandoned solution (source), if exists, and replace it with a new randomly produced solution $\mathbf{x}_i$ for the scout using the following equation:

$$x_{i,j} = x_{\min,j} + \mathrm{rand}(0,1)\left(x_{\max,j} - x_{\min,j}\right). \tag{4}$$

(8) Memorize the position of the best food source found so far.

(9) Repeat the procedure from step (3) till the termination criterion is met.

It should be noted that if the components of the candidate food position $\mathbf{v}_i$ violate the predefined constraints, a simple method is used to set the violating components to be the middle of the violated bounds and the corresponding components of the old $\mathbf{x}_i$, as follows:

$$\begin{aligned} v_{i,j} &= \frac{x_{\min,j} + x_{i,j}}{2} \quad \text{if } v_{i,j} < x_{\min,j}, \\ v_{i,j} &= \frac{x_{\max,j} + x_{i,j}}{2} \quad \text{if } v_{i,j} > x_{\max,j}. \end{aligned} \tag{5}$$

3. Sequential Kriging Optimization (SKO)

3.1. The Basics of Kriging Model. The advantage of ABC algorithm mentioned above is that it more likely converges to the global optimum. However, like other population-based algorithms, ABC needs a greater number of objective evaluations to converge, which is closely related to the computational time. To address this issue, the metamodeling or surrogate modeling technique was used in this paper. The surrogate model can provide an approximate functional relationship to relate design variables to specific responses with a moderate number of full computational analyses. In practice, the first step of constructing surrogate modeling is to generate the sampling data (training points). Design of experiment (DoE) is an approach to addressing how to select training points effectively. In this paper, the optimal Latin hypercube sampling (OLHS) [25, 26] is implemented to generate initial training points.

After generating training points, various metamodeling methods, namely, polynomial response surface (PRS), moving least square (MLS), Kriging (KRG), and radial basis function (RBF), can been implemented for approximation of the performance responses. The Kriging model is chosen herein mainly because (1) it allows better capturing of nonlinear response with respect to spot weld locations and (2) the predicted error of its estimated response value can be easily obtained as a by-product that will form a basis of sequential sampling strategy to be outlined below.

The Kriging model was originally developed for mining and geostatistical applications involving spatially and temporally correlated data [27]. The Kriging model assumes the deterministic response of a system to be a stochastic process function $y(\mathbf{x})$, consisting of a regression model and a stochastic error [28]:

$$y(\mathbf{x}) = \mathbf{f}(\mathbf{x})^{\mathrm{T}}\boldsymbol{\beta} + z(\mathbf{x}), \tag{6}$$

where $\boldsymbol{\beta}$ is the column vector of regression parameters, $\boldsymbol{\beta} = [\beta_1, \beta_2, \ldots, \beta_p]^{\mathrm{T}}$; $\mathbf{f}(\mathbf{x})$ is the column vector of basis functions, $\mathbf{f}(\mathbf{x}) = [f_1(\mathbf{x}), f_2(\mathbf{x}), \ldots, f_p(\mathbf{x})]^{\mathrm{T}}$; p denotes the number of basis functions; $z(\mathbf{x})$ represents a stochastic parameter with zero mean, variance σ^2, and nonzero covariance. The covariance matrix of $z(\mathbf{x})$ is given as

$$\mathrm{Cov}\left[z(\mathbf{x}_i), z(\mathbf{x}_j)\right] = \sigma^2 \mathbf{R}\left[R(\mathbf{x}_i, \mathbf{x}_j)\right], \tag{7}$$

where $\mathbf{R}$ is a correlation matrix defined by Gaussian correlation function $R(\mathbf{x}_i, \mathbf{x}_j)$ as follows:

$$R(\mathbf{x}_i, \mathbf{x}_j) = \exp\left[-\sum_{k=1}^{N} \theta_k \left|x_{i,k} - x_{j,k}\right|^2\right], \tag{8}$$

where θ_k is the unknown correlation parameter used to fit the model.

Then, the predicted estimate $\hat{y}(\mathbf{x})$ of response $y(\mathbf{x})$ is given as

$$\hat{y}(\mathbf{x}) = \mathbf{f}(\mathbf{x})^{\mathrm{T}}\hat{\boldsymbol{\beta}} + \mathbf{r}^{\mathrm{T}}(\mathbf{x})\mathbf{R}^{-1}\left(\mathbf{y}_s - \mathbf{F}\hat{\boldsymbol{\beta}}\right), \tag{9}$$

where $\mathbf{y}_s = [y(\mathbf{x}_1), y(\mathbf{x}_2), \ldots, y(\mathbf{x}_{n_s})]^{\mathrm{T}}$ is the response vector of the n_s training points $\mathbf{x}_s = \{\mathbf{x}_1, \mathbf{x}_2, \ldots, \mathbf{x}_{n_s}\}$ which are obtained from the finite element analyses, and $\mathbf{F} = [\mathbf{f}(\mathbf{x}_1), \mathbf{f}(\mathbf{x}_2), \ldots, \mathbf{f}(\mathbf{x}_{n_s})]^{\mathrm{T}}$ is an $n_s \times p$ matrix. $\mathbf{r}^{\mathrm{T}}(\mathbf{x}) = [R(\mathbf{x}, \mathbf{x}_1), R(\mathbf{x}, \mathbf{x}_2), \ldots, R(\mathbf{x}, \mathbf{x}_{n_s})]^{\mathrm{T}}$ is a correction vector that implies how close it is between training points and untried points. $\widehat{\boldsymbol{\beta}}$ is the general least square estimator given as follows:

$$\widehat{\boldsymbol{\beta}} = \left(\mathbf{F}^{\mathrm{T}}\mathbf{R}^{-1}\mathbf{F}\right)^{-1}\mathbf{F}^{\mathrm{T}}\mathbf{R}^{-1}\mathbf{y}_s. \tag{10}$$

The estimate to the variance of training data from the global model is

$$\widehat{\sigma}^2 = \frac{\left(\mathbf{y}_s - \mathbf{F}\widehat{\boldsymbol{\beta}}\right)^{\mathrm{T}}\mathbf{R}^{-1}\left(\mathbf{y}_s - \mathbf{F}\widehat{\boldsymbol{\beta}}\right)}{n_s}. \tag{11}$$

For calculating θ_k in (8), the maximum likelihood estimates can be used by solving the following the maximization problem over the interval $\theta_k > 0$, as

$$\max\left(-\frac{n_s \ln\left(\widehat{\sigma}^2\right) + \ln|\mathbf{R}|}{2}\right), \tag{12}$$

where both $\widehat{\sigma}^2$ and $|\mathbf{R}|$ are the functions of θ_k.

Kriging model provides estimation to the prediction error from an unobserved point, which is also called the mean squared error (MSE):

$$\widehat{s}^2(\mathbf{x}) = \widehat{\sigma}^2\left\{1 - \left[\mathbf{f}^{\mathrm{T}}(\mathbf{x})\,\mathbf{r}^{\mathrm{T}}(\mathbf{x})\right]\begin{bmatrix}\mathbf{0} & \mathbf{F}^{\mathrm{T}}\\ \mathbf{F} & \mathbf{R}\end{bmatrix}^{-1}\begin{bmatrix}\mathbf{f}(\mathbf{x})\\ \mathbf{r}(\mathbf{x})\end{bmatrix}\right\}. \tag{13}$$

In this study, we adopt the ordinary Kriging model [29], in which the regression can be reduced to a simple constant term (i.e., $\mathbf{f}(\mathbf{x})^{\mathrm{T}}\boldsymbol{\beta} = \boldsymbol{\beta}$) without significant loss in model fidelity. As a result, $\mathbf{F}$ turns out to be a column vector filled with unity.

3.2. Sequential Improvement. Several previous investigations [30–38] have shown certain advantages provided by a particular sequential sampling strategy. Therefore, in order to further reduce the number of FEA, the paper also combined Kriging modeling with sequential sampling strategy to optimize the spot-welded joints, which was referred to as sequential Kriging optimization (SKO) or efficient global optimization (EGO) in the literature.

As abovementioned, the Kriging model allows predicting two important parts of response, (1) an approximation to the objective ($\widehat{y}(\mathbf{x})$ in (9)) and (2) an estimate of the mean squared error (MSE, i.e., $\widehat{s}^2(\mathbf{x})$ as in (13)) at the untried point. The sequential improvement strategy adopted here was proposed by Schonlau [38]. This method starts by defining improvement I:

$$I = \begin{cases} f_{\min} - y & \text{if } y < f_{\min} \\ 0 & \text{otherwise,} \end{cases} \tag{14}$$

where $f_{\min}$ is the lowest objective function value obtained during previous iterations and y is a possible new outcome of a function evaluation. Clearly, if $y < f_{\min}$, the situation has improved. The expected value of a stochastic variable X is defined as

$$E(X) = \int_{-\infty}^{\infty} x p(x)\, dx \tag{15}$$

in which x is a possible value of X and $p(x)$ is the probability that X actually has the value of x. Assuming a normal distribution, the expected improvement can be obtained by substituting (14) into (15):

$$E(I) = \int_{-\infty}^{f_{\min}} \left(f_{\min} - y\right)\varphi(y)\, dy, \tag{16}$$

where $\varphi(y)$ is the normal probability density function. Now y can be replaced by the Kriging prediction value $\widehat{y}(\mathbf{x})$ and (16) can be rewritten to

$$E(I) = \left(f_{\min} - \widehat{y}(\mathbf{x})\right)\Phi\left(\frac{f_{\min} - \widehat{y}(\mathbf{x})}{\widehat{s}(\mathbf{x})}\right) + \widehat{s}(\mathbf{x})\,\phi\left(\frac{f_{\min} - \widehat{y}(\mathbf{x})}{\widehat{s}(\mathbf{x})}\right), \tag{17}$$

where $\phi(\cdot)$ and $\Phi(\cdot)$ denote the probability density and the cumulative distribution functions of the standard normal distribution. Schonlau [38] proposed to maximize $E(I)$ to yield the point promising the maximum expected improvement (MEI). This maximization optimization problem was solved by ABC in this paper. In addition, at each iteration the global optimum was sought by running ABC based on the established Kriging model and then checking the accuracy by FEA. And this point was added to the training dataset for the Kriging refitting of next iteration, as well as the MEI point. To address the local clustering, the new training points were filtered according to their distance to other points and the inappropriate points were removed from the dataset. The sequential sampling and optimization cycle terminates when the error at the optimum point between the Kriging prediction value and FEA value becomes very small (e.g., <1%). Figure 1 summarizes the whole process of SKO for clarification.

4. Optimization Problem of Spot-Welded Plates

4.1. Finite Element Modeling. The spot-welded structure studied herein was a tensile-shear joint of two plates, whose geometry is depicted in Figure 2. The dimensions of the plates are 100 × 50 × 1.0 mm, their overlapping length is 50 mm, and the diameters of the spot welds are 4 mm. For obtaining accurate results of stress and strain states developed in the structure, commercial FEA software ANSYS was utilized. A 3D ten-node tetrahedral solid element (SOLID 92) was used for the plates. This element has plasticity, stress stiffening, large deflection, and large strain capabilities. Each spot weld set consisted of a beam element and two node-to-surface MPC contact pairs. The nugget was modeled using a two-node beam element (BEAM 188), which linked the spot weld surfaces. Each contact pair has only one contact element (CONTA175) which is defined by the associated spot weld node. The target elements (TARGE170) were formed by a group of surface nodes lying within the search radius, which was set four times the spot weld radius. Six constraint equations were generated for each spot weld surface (i.e., each contact pair) by the software capacity to couple the motion of

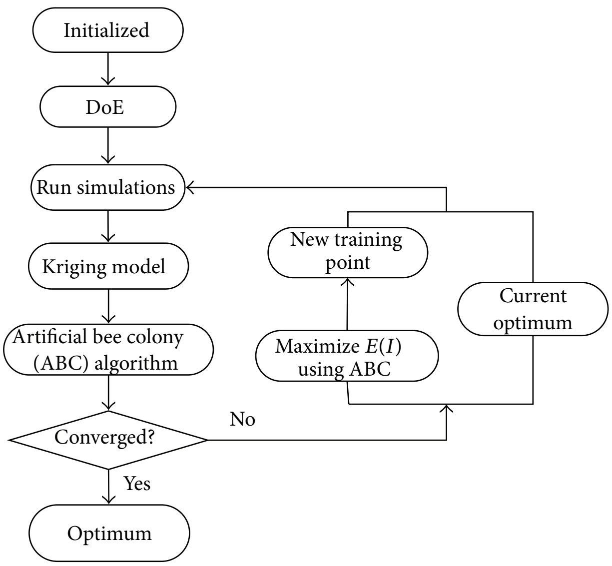

Figure 1: Flowchart of hybrid optimization combined SKO with ABC.

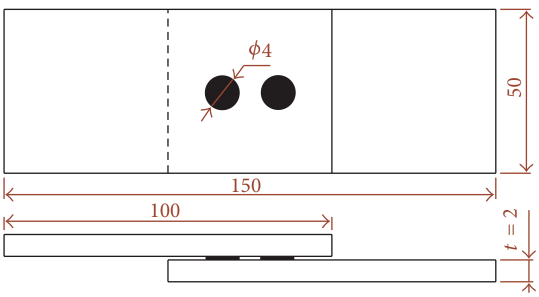

Figure 2: Geometry of the TS specimen.

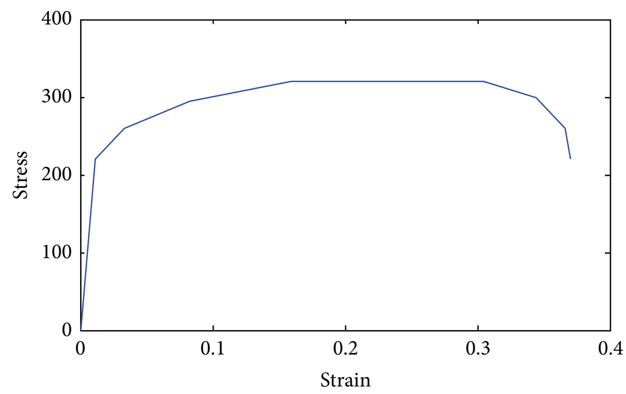

Figure 3: Engineering stress-strain curve.

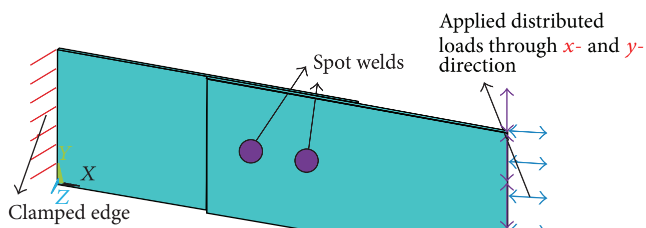

Figure 4: Boundary conditions.

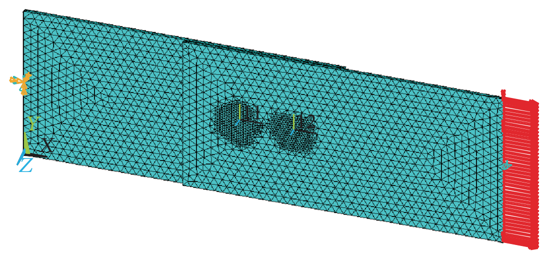

Figure 5: Finite element model.

contact nodes to the motion of the target node in an average sense.

In addition to the contact condition, nonlinearity in material property and geometry deformation were also considered in this study. The basic material property was generated on the basis of the engineering stress versus strain through

$$\sigma = S(1+e),$$
$$\varepsilon = \ln(1+e), \quad (18)$$

where S and e are engineering stress and strain, respectively, and σ and ε are the true stress and strain, respectively. The engineering stress versus strain curve for the basic plates was depicted in Figure 3, and the elastic properties were set as $E = 207$ GPa and $\nu = 0.25$. Because the nugget develops low stress, its material model was selected as linearly elastic. As heat treatment does not cause an appreciable change in elastic modulus and Poisson's ratio, their magnitudes were considered to remain about the same throughout the specimen despite melting during the formation of the nugget.

The boundary condition of the FE model is shown in Figure 4. All of the six translational and rotational degrees of freedom were constrained at one end. The other end was subjected to uniformly distributed in-plane loads in the x-direction and y-direction (1000 N and 250 N, resp.), while the displacement was prevented in the z-direction. Due to high stress concentration, much smaller elements were used around the spot-weld nuggets in comparison to those of the base metal as shown in Figure 5.

Figures 6(a) and 6(b) show equivalent stress distribution (in terms of Mega Pascal) over the inner surfaces of the lower and upper sheets, respectively. High stresses develop at regions on the inner surfaces of the sheets close to the peripheries of the spot welds because load transfer in a spot-weld nugget mainly occurs through the material near the boundary of the nugget, whilst the central region of the nugget bears relatively low stresses.

4.2. Description of Optimization Problem. In this paper, we aim to maximize the fatigue life for a spot-welded structure. The absolute maximum principal strain theory of multiaxial

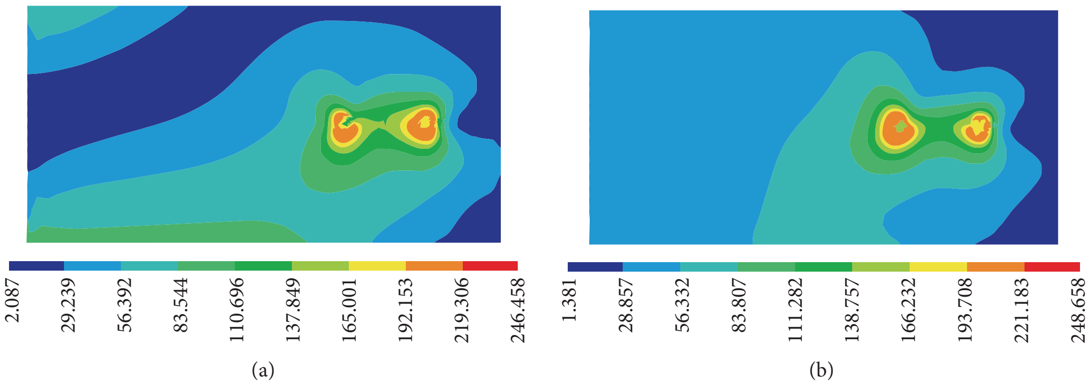

FIGURE 6: Von Mises stress distrubition on inner surfaces of the initial design: (a) lower sheet; (b) upper sheet.

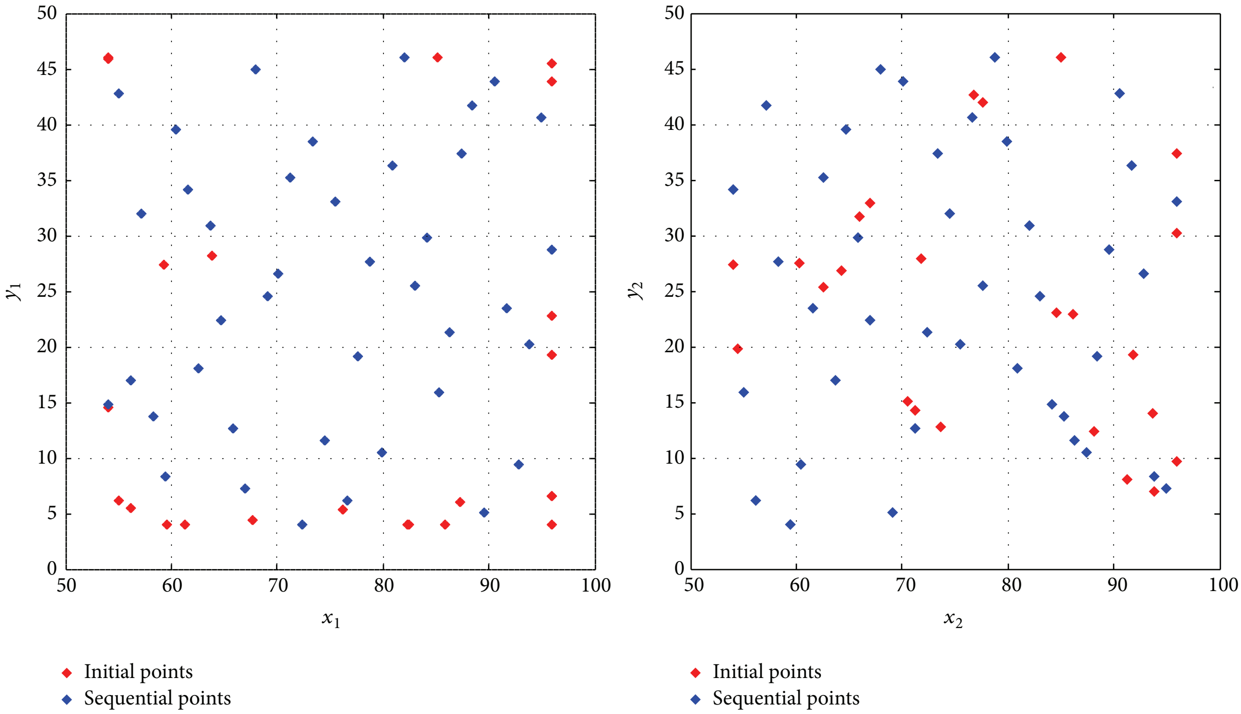

FIGURE 7: Distribution of DoE points.

fatigue failure proposed by Ellyin and Valaire [39] states that similar fatigue lives will be achieved when the maximum principal strains are the same. Pan and Sheppard [3] also drew similar conclusion that the maximum principal strain is able to correlate well with fatigue life for spot-welded joints. Hence the maximum principal strain was used as the objective to characterize the fatigue behavior of spot welds in this study.

The spot welds should be allocated properly to avoid interfering with each other and getting close to the plate boundaries. That is to say, the design should conform to the standards related to weld-to-weld spacing and weld-to-edge distance. According to American Welding Society, the distance between an edge and the center of a spot weld should be greater than one spot weld diameter. Besides, the distance between the centers of the spot welds should be greater than twice the spot-weld diameter as recommended by the industry. As a result, the mathematical problem to be optimized regarding the spot weld locations can be formulated as

$$\begin{aligned} &\min \quad \varepsilon_1 \\ &\text{s.t.} \quad D = \sqrt{(x_1 - x_2)^2 + (y_1 - y_2)^2} \geq 2d \\ &\qquad 50 + d \leq x_1, \quad x_2 \leq 100 - d \\ &\qquad d \leq y_1, \quad y_2 \leq 50 - d, \end{aligned} \tag{19}$$

where ε_1 denotes the maximum principal strain, D represents the distance between the spot welds, d is the diameter of the spot weld (herein $d = 4$), and x_1 and y_1 are the center

Table 1: Initial DoE points and their FEA results.

Number	x_1	y_1	x_2	y_2	ε_1	D
1	54.00	14.77	88.46	19.08	0.00230	34.73
2	55.08	42.77	74.46	32.00	0.05778	22.17
3	56.15	16.92	72.31	21.23	0.02341	16.72
4	57.23	32.00	58.31	27.69	—	4.44
5	58.31	13.69	76.62	40.62	0.00951	32.57
6	59.38	8.31	85.23	13.69	0.00170	26.40
7	60.46	39.54	86.31	11.54	0.00518	38.11
8	61.54	34.15	71.23	12.62	0.02314	23.61
9	62.62	18.00	90.62	42.77	0.00768	37.38
10	63.69	30.92	62.62	35.23	—	4.44
11	64.77	22.31	63.69	16.92	—	5.50
12	65.85	12.62	57.23	41.69	0.01500	30.32
13	66.92	7.23	73.38	37.38	0.00545	30.83
14	68.00	44.92	68.00	44.92	—	0.00
15	69.08	24.46	59.38	4.00	0.00459	22.64
16	70.15	26.62	84.15	14.77	0.01945	18.34
17	71.23	35.23	82.00	30.92	0.22667	11.60
18	72.31	4.00	55.08	15.85	0.00468	20.91
19	73.38	38.46	69.08	5.08	0.00683	33.66
20	74.46	11.54	93.85	8.31	0.00180	19.66
21	75.54	33.08	54.00	34.15	0.06039	21.57
22	76.62	6.15	77.69	25.54	0.00513	19.42
23	77.69	19.08	80.92	18.00	—	3.41
24	78.77	27.69	66.92	22.31	0.05791	13.01
25	79.85	10.46	92.77	26.62	0.00357	20.69
26	80.92	36.31	94.92	7.23	0.00369	32.27
27	82.00	46.00	79.85	38.46	—	7.84
28	83.08	25.54	56.15	6.15	0.00340	33.18
29	84.15	29.85	96.00	33.08	0.07518	12.28
30	85.23	15.85	64.77	39.54	0.01403	31.30
31	86.31	21.23	78.77	46.00	0.02269	25.89
32	87.38	37.38	60.46	9.38	0.00353	38.84
33	88.46	41.69	89.54	28.77	0.15530	12.97
34	89.54	5.08	87.38	10.46	—	5.80
35	90.62	43.85	75.54	20.15	0.01949	28.09
36	91.69	23.38	91.69	36.31	0.06770	12.93
37	92.77	9.38	61.54	23.38	0.00249	34.22
38	93.85	20.15	65.85	29.85	0.00567	29.63
39	94.92	40.62	70.15	43.85	0.06428	24.98
40	96.00	28.77	83.08	24.46	0.04458	13.62

coordinates in the x-direction and y-direction for the first spot weld, respectively, and x_2 and y_2 for the second spot weld, respectively. In this study, penalty method is employed to handle the constraints

5. Results and Discussions

Table 1 lists the initial DoE sample points generated using OLHS, and its size is chosen 10 times the number of the variables (i.e., 40). Figure 7 displays the distribution of the sample points over the design space, from which it is easily found that the initial DoE points are generated evenly. Therefore, these sample points can extract the overall trend of the objective and lay a foundation for obtaining a global optimum in the subsequent optimization process.

From Table 1, 7 points violate the distance constraint and thus are not further submitted to analyzer (ANSYS) for calculating stress and strain states. After generating the initial DoE points, the iterations of sequential sampling begin to work according to Figure 1, and the majority of the newly

Table 2: Sequential DoE points and their FEA results.

Number	x_1	y_1	x_2	y_2	ε_1	D
1	96.00	45.52	71.27	14.21	0.00635	39.90
2	96.00	43.85	70.59	15.04	0.00656	38.41
3	67.67	4.35	84.99	46.00	0.00569	45.10
4	85.15	46.00	73.62	12.74	0.00635	35.20
5	59.24	27.39	93.75	6.94	0.00255	40.11
6	63.90	28.14	91.20	7.98	0.00315	33.94
7	96.00	4.00	67.02	32.88	0.00305	40.92
8	96.00	6.49	66.05	31.64	0.00286	39.11
9	82.35	4.00	91.88	19.27	0.00209	18.00
10	96.00	22.72	54.00	27.39	0.00311	42.26
11	96.00	19.21	60.29	27.56	0.00301	36.68
12	76.27	5.40	96.00	37.39	0.00318	37.58
13	85.93	4.00	71.79	27.90	0.00346	27.77
14	54.00	46.00	62.63	25.34	0.07214	22.39
15	96.00	6.53	84.58	23.02	0.00249	20.06
16	87.22	6.04	86.09	22.93	0.00256	16.93
17	61.31	4.00	76.80	42.62	0.00410	41.62
18	59.60	4.00	77.62	41.94	0.00406	42.00
19	54.00	45.94	54.42	19.86	0.04015	26.09
20	54.00	14.47	96.00	9.71	0.00165	42.27
21	82.52	4.00	96.00	30.18	0.00289	29.45
22	55.10	6.16	93.72	13.94	0.00166	39.39
23	54.00	46.00	64.24	26.85	0.09402	21.71
24	56.11	5.44	88.18	12.34	0.00164	32.80

generated points are located on the boundary of the design space as shown in Figure 7. This is because large prediction uncertainties exist in those areas, and adding sample points there can effectively enhance the expected improvement. Finally, after 12 iterations the process becomes converged. Table 2 provides the iteration history of the sequential sampling, where the constraint is actually inactive during the whole iteration and the objective has a lower average value compared to that of the initial samples.

Overall, the FEA is executed 57 times for yielding the global optimum in our proposed optimization process. The resulting maximum principal strain is reduced significantly compared to the initial design (as listed in Table 3), which indicates that the fatigue life can be improved considerably through optimization. Besides, the optimal locations are fairly different from the initial ones, signifying the importance of optimization. The first spot weld moves to one corner of the overlapping square area of sheets, and the second one also moves to the boundary of this area. Figures 8(a) and 8(b) display the equivalent stress distribution on the inner surfaces of optimized design, where the maximum value is reduced to around 221 MPa from the original value 249 MPa.

To validate the effectiveness of our proposed method, the conventional optimizations directly coupling with FEA model were also done and the results are also listed in Table 3, where Nelder-Mead simplex method and sequential quadratic programming (SQP) were adapted for comparison. It is known that the selection of starting point can affect the optimization results when using the two algorithms. Because the objective is a complex function of spot weld positions, it is difficult to choose the starting point according to the engineering experience. Thus, the initial design is used as the starting point for both Nelder-Mead method and SQP. From Table 3, we can see that both directly coupling methods converge to local minima near the initial design, although SQP calls fewer FEA than SKO. They might be able to find a global optimum by executing the algorithms many times starting from different initial points. However, it will definitely increase the computational time and cost significantly. On the other hand, our proposed method enables us to find more optimal locations for spot welds in terms of the fatigue life with a relatively low computational burden.

Table 3: Initial design, optimum obtained from ABC-SKO, and comparison with other methods.

	Initial design	ABC-SKO	Simplex	SQP
x_1	67.00	55.10	63.45	67.21
y_1	25.00	6.16	28.53	25.12
x_2	84.00	93.72	86.53	84.44
y_2	25.00	13.94	44.65	25.11
ε_1	0.0396	0.00165	0.0262	0.0251
Number of FEA	—	57	79	34

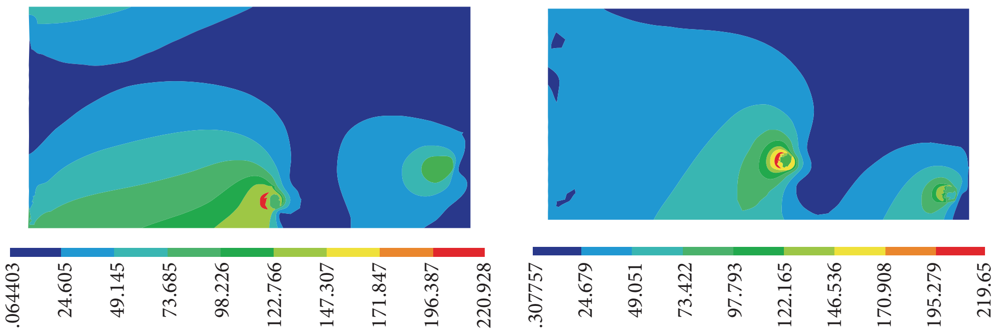

(a) (b)

Figure 8: Von Mises stress distrubition on inner surfaces of the optimized design: (a) lower sheet; (b) upper sheet.

6. Conclusion

To efficiently improve the fatigue life of spot-welded structure, a metamodel-based optimization procedure is proposed, which integrates finite element analysis (FEA), ABC with SKO. The Kriging model is first established to approximate the relationship between the maximum principal strain of the spot-welded joint and the locations of the spot welds, based on the initial training points generated by the optimal Latin hypercube sampling (OLHS) scheme. Then the sequential sampling strategy and ABC are implemented to run the optimization, where the point promising the maximum expected improvement (MEI) and the current global optimum obtained from ABC based on the Kriging model are taken as the new training points. After that, the Kriging model is updated and the optimization process continues to the next iteration until the stopping criteria are satisfied. To validate the effectiveness of our optimization procedure, the comparison with other methods is conducted. The results show that the proposed method can significantly enhance the fatigue performance of the spot-welded joints with a low number of FEA.

Conflict of Interests

The authors declare that there is no conflict of interests regarding the publication of this paper.

Acknowledgments

This work was supported by the National 973 Project of China (2011CB711205), the National Natural Science Foundation of China (11202072), the Hunan Provincial Science Foundation of China (13JJ4036), and the Doctoral Fund of Ministry of Education of China (20120161120005). The first author is a recipient of the doctoral scholarships from both China Scholarship Council (CSC) and the University of Sydney.

References

[1] A. H. Ertas and F. O. Sonmez, "Design optimization of spot-welded plates for maximum fatigue life," *Finite Elements in Analysis and Design*, vol. 47, no. 4, pp. 413–423, 2011.

[2] X. Deng, W. Chen, and G. Shi, "Three-dimensional finite element analysis of the mechanical behavior of spot welds," *Finite Elements in Analysis and Design*, vol. 35, no. 1, pp. 17–39, 2000.

[3] N. Pan and S. Sheppard, "Spot welds fatigue life prediction with cyclic strain range," *International Journal of Fatigue*, vol. 24, no. 5, pp. 519–528, 2002.

[4] S. Mahadevan and K. Ni, "Damage tolerance reliability analysis of automotive spot-welded joints," *Reliability Engineering and System Safety*, vol. 81, no. 1, pp. 9–21, 2003.

[5] R. J. Wang and D. G. Shang, "Low-cycle fatigue life prediction of spot welds based on hardness distribution and finite element analysis," *International Journal of Fatigue*, vol. 31, no. 3, pp. 508–514, 2009.

[6] A. H. Ertas, O. Vardar, F. O. Sonmez, and Z. Solim, "Measurement and assessment of fatigue life of spot-weld joints," *Journal of Engineering Materials and Technology, Transactions of the ASME*, vol. 131, no. 1, Article ID 0110111, 11 pages, 2009.

[7] R. Tovo and P. Livieri, "A numerical approach to fatigue assessment of spot weld joints," *Fatigue and Fracture of Engineering Materials and Structures*, vol. 34, no. 1, pp. 32–45, 2011.

[8] Y. Zhang and D. Taylor, "Optimization of spot-welded structures," *Finite Elements in Analysis and Design*, vol. 37, no. 12, pp. 1013–1022, 2001.

[9] S. W. Chae, K. Y. Kwon, and T. S. Lee, "An optimal design system for spot welding locations," *Finite Elements in Analysis and Design*, vol. 38, no. 3, pp. 277–294, 2002.

[10] A. H. Ertas and F. O. Sonmez, "Optimization of spot-weld joints," *Proceedings of the Institution of Mechanical Engineers C: Journal of Mechanical Engineering Science*, vol. 223, no. 3, pp. 545–555, 2009.

[11] R. J. Yang, N. Wang, C. H. Tho, J. P. Bobineau, and B. P. Wang, "Metamodeling development for vehicle frontal impact simulation," *Journal of Mechanical Design*, vol. 127, no. 5, pp. 1014–1020, 2005.

[12] J. Fang, Y. Gao, G. Sun, Y. Zhang, and Q. Li, "Parametric analysis and multiobjective optimization for functionally graded foam-filled thin-wall tube under lateral impact," *Computational Materials Science*, vol. 90, pp. 265–275, 2014.

[13] X. G. Song, J. H. Jung, H. J. Son, J. H. Park, K. H. Lee, and Y. C. Park, "Metamodel-based optimization of a control arm considering strength and durability performance," *Computers and Mathematics with Applications*, vol. 60, no. 4, pp. 976–980, 2010.

[14] J. Fang, Y. Gao, G. Sun, and Q. Li, "Multiobjective reliability-based optimization for design of a vehicle door," *Finite Elements in Analysis and Design*, vol. 67, pp. 13–21, 2013.

[15] G. Y. Sun, G. Y. Li, and Q. Li, "Variable fidelity design based surrogate and artificial bee colony algorithm for sheet metal forming process," *Finite Elements in Analysis and Design*, vol. 59, pp. 76–90, 2012.

[16] D. Karaboga and B. Akay, "A comparative study of artificial Bee colony algorithm," *Applied Mathematics and Computation*, vol. 214, no. 1, pp. 108–132, 2009.

[17] M. Sonmez, "Artificial bee colony algorithm for optimization of truss structures," *Applied Soft Computing Journal*, vol. 11, no. 2, pp. 2406–2418, 2011.

[18] D. Karaboga, C. Ozturk, N. Karaboga, and B. Gorkemli, "Artificial bee colony programming for symbolic regression," *Information Sciences*, vol. 209, pp. 1–15, 2012.

[19] D. Karaboga and B. Akay, "A survey: algorithms simulating bee swarm intelligence," *Artificial Intelligence Review*, vol. 31, no. 1–4, pp. 61–85, 2009.

[20] D. Karaboga, B. Gorkemli, C. Ozturk, and N. Karaboga, "A comprehensive survey: artificial bee colony (ABC) algorithm and applications," *Artificial Intelligence Review*, vol. 42, pp. 21–57, 2014.

[21] D. Karaboga, "An idea based on honey bee swarm for numerical optimization," Technical Report tr06, Computer Engineering Department, Engineering Faculty, Erciyes University, 2005.

[22] D. Karaboga, "Artificial bee colony algorithm," *Scholarpedia*, vol. 5, no. 3, article 6915, 2010.

[23] D. Karaboga and B. Basturk, "A powerful and efficient algorithm for numerical function optimization: artificial bee colony (ABC) algorithm," *Journal of Global Optimization*, vol. 39, no. 3, pp. 459–471, 2007.

[24] D. Karaboga and B. Basturk, "On the performance of artificial bee colony (ABC) algorithm," *Applied Soft Computing Journal*, vol. 8, no. 1, pp. 687–697, 2008.

[25] R. Jin, W. Chen, and A. Sudjianto, "An efficient algorithm for constructing optimal design of computer experiments," *Journal of Statistical Planning and Inference*, vol. 134, no. 1, pp. 268–287, 2005.

[26] K. Sinha, "Reliability-based multiobjective optimization for automotive crashworthiness and occupant safety," *Structural and Multidisciplinary Optimization*, vol. 33, no. 3, pp. 255–268, 2007.

[27] J. Sacks, W. J. Welch, T. J. Mitchell, and H. P. Wynn, "Design and analysis of computer experiments," *Statistical Science*, vol. 4, no. 4, pp. 409–423, 1989.

[28] Y. Gao and F. Sun, "Multi-disciplinary optimisation for front auto body based on multiple optimisation methods," *International Journal of Vehicle Design*, vol. 57, no. 2-3, pp. 178–195, 2011.

[29] M. J. Sasena, *Flexibility and efficiency enhancements for constrained global design optimization with kriging approximations [Ph.D. thesis]*, University of Michigan, Ann Arbor, Mich, USA, 2002.

[30] D. R. Jones, M. Schonlau, and W. J. Welch, "Efficient global optimization of expensive black-box functions," *Journal of Global Optimization*, vol. 13, no. 4, pp. 455–492, 1998.

[31] A. J. Booker, J. E. Dennis Jr., P. D. Frank, D. B. Serafini, V. Torczon, and M. W. Trosset, "A rigorous framework for optimization of expensive functions by surrogates," *Structural Optimization*, vol. 17, no. 1, pp. 1–13, 1999.

[32] M. J. Sasena, P. Papalambros, and P. Goovaerts, "Exploration of metamodeling sampling criteria for constrained global optimization," *Engineering Optimization*, vol. 34, no. 3, pp. 263–278, 2002.

[33] D. Huang, T. T. Allen, W. I. Notz, and R. A. Miller, "Sequential kriging optimization using multiple-fidelity evaluations," *Structural and Multidisciplinary Optimization*, vol. 32, no. 5, pp. 369–382, 2006.

[34] D. Huang, T. T. Allen, W. I. Notz, and N. Zeng, "Global optimization of stochastic black-box systems via sequential kriging meta-models," *Journal of Global Optimization*, vol. 34, no. 3, pp. 441–466, 2006.

[35] F. Xiong, Y. Xiong, W. Chen, and S. Yang, "Optimizing latin hypercube design for sequential sampling of computer experiments," *Engineering Optimization*, vol. 41, no. 8, pp. 793–810, 2009.

[36] M. H. A. Bonte, L. Fourment, T. T. Do, A. H. van den Boogaard, and J. Huétink, "Optimization of forging processes using finite element simulations : a comparison of sequential approximate optimization and other algorithms," *Structural and Multidisciplinary Optimization*, vol. 42, no. 5, pp. 797–810, 2010.

[37] S. Kitayama, M. Arakawa, and K. Yamazaki, "Sequential approximate optimization using radial basis function network for engineering optimization," *Optimization and Engineering*, vol. 12, no. 4, pp. 535–557, 2011.

[38] M. Schonlau, *Computer experiments and global optimization [Ph.D. thesis]*, University of Waterloo, Ontario, Canada, 1997.

[39] F. Ellyin and B. Valaire, "High-strain multiaxial fatigue. Journal of Engineering Materials and Technology," *Journal of Engineering Materials and Technology*, vol. 104, no. 3, pp. 165–173, 1982.